Numerical validation of a DeepCwind floating platform with inclined taut-legs under regular waves using the SPH method

Numerical validation of a DeepCwind floating platform with inclined taut-legs under regular waves using the SPH method

B. Tagliafierro
Maritime Engineering laboratory, Universitat Politècnica de Catalunya – BarcelonaTech, Barcelona, Spain
School of Natural and Built Environment, Queen's University Belfast, Belfast, United Kingdom

S. Capasso & G. Viccione
Environmental and Maritime Hydraulics Laboratory (LIDAM), University of Salerno, Italy

O. Dell'Edera & F. Niosi
Politecnico di Torino, MOREnergy Lab, DIMEAS, Turin, Italy

I. Martínez-Estévez & J. Domínguez
Environmental Physics Laboratory, CIM-UVIGO Universidade de Vigo, Ourense, Spain

M. Göteman
Dept. of Electrical Engineering, Uppsala University, Uppsala Sweden

M. Karimirad
School of Natural and Built Environment, Queen's University Belfast, Belfast, United Kingdom

ABSTRACT: Hydrodynamic investigation and characterization of floating offshore wind turbine platforms has gained substantial research attention. In this study, we perform a numerical investigation using an SPH-based tool to identify the frequency properties of a DeepCwind platform equipped with a system of inclined, taut mooring lines. An open dataset is used as a reference solution: a DeepCwind-like platform tested using the semi-submersible layout proposed during the OC5 experimental campaign. The platform was kept at station by a system of inclined, pre-tensioned lines. Here, the model is validated against a decay test and response amplitude operators. It has shown good performance, indicating its capability in capturing second-order effects.

1 INTRODUCTION

As the offshore wind market steadily grows in investments and breadth, likewise research effort is poured into the development of reliable design tools, facilitating the prediction of floating offshore wind turbines (FOWTs) performance in highly energetic seas (Lauria et al., 2024). Despite having comprehensive models, such as OpenFAST (Jonkman, Buhl, et al., 2005) able to account at once for the broad variety of environmental loads, i.e., wind, currents, waves, and even their structural effects, i.e., column swinging, and aero-elasticity, the accuracy of the hydrodynamic modeling, which often relies on model calibration (Niosi et al., 2023c), has emerged as a critical metric to evaluate a model usability (Faraggiana et al., 2022). Nonlinear hydrodynamic loads and second-order effects appear (Antonutti et al., 2014; Shi et al., 2023) to trigger the response of floating platform out of the prediction of low- or mid-fidelity models, with significant consequences on the frequency properties estimation. It goes that our numerical instruments underwent a substantial bottom-to-up inspection, shifting the research interest in correctly anticipating the hydrodynamics of such complex structural units. Systemic research carried out by the Offshore Code Comparison Collaboration Continued with Correlation (OC5 – Robertson et al. (2017)) has highlighted a *persistent underprediction* in load and motion magnitudes by engineering tools used during the restitution phase. The research posits that the misrepresentation of low-frequency loads may stem from in-

accurate fluid resolution (Robertson et al., 2020).

Computational fluid dynamics (CFD)-based numerical environments, instead, are designed to realistically capture flow features, including viscous wave-to-structure actions, and, most importantly, structure-to-wave response (Zhang et al., 2024). Integrating these realistic features within the core of the design process appears to be the most suitable solution to enhance the wave–structure interaction (WSI) reproduction. Such frameworks bear great potential to evaluate structure performance under extreme conditions, as revealed for wave energy converter interactions with waves (Ransley et al., 2017; Windt et al., 2018; Davidson & Costello, 2020; Tagliafierro et al., 2022b; Katsidoniotaki et al., 2023; Paduano et al., 2024; Crespo et al., 2023). Consequently, the ensuing Offshore Code Comparison Collaboration, Continued with Correlation, and unCertainty (OC6) project aimed to assess the sources of inaccuracy and perform more focused investigations to improve the general credibility of CFD methods through validation (see, regarding OCX projects results Wang et al., 2022; Wang et al., 2021; Robertson & Wang, 2021).

The family of CFD models includes a broad range of solvers, with peculiar characteristics and functioning that can make them more or less suitable for these challenges. Navier–Stokes solvers based on the meshless Smoothed Particle Hydrodynamics (SPH) method, notably, exhibit interesting features for WSI simulations, as their Lagrangian nature inherently allows for moving boundaries treatment and consistent fluid deformation, also overcoming grid-related numerical issues, such as distortions or inconsistent boundary interfaces. In previous work by the authors (Tagliafierro et al., 2023b), along with establishing an SPH-based numerical environment for end-to-end platform hydrodynamic design, a comprehensive state of the art for SPH models of FOWTs is proposed; what certainly stands out is the flexibility of such approaches and their encouraging rate of development, along with the wide possibilities of further extend the accounted physics with internal or external structural couplings (see Tan et al. (2023), Pribadi et al. (2023), Tagliafierro et al. (2023a), or Salis et al. (2024), among others). In Tagliafierro et al. (2023c), for instance, wind turbulence models are included as forcing conditions on a TLP-like platform (Tagliafierro et al., 2022a), proving that critical dynamics, as surge springing, is enhanced when coupled wind-wave actions are considered in a fully nonlinear environment.

The numerical tool adopted in the investigations reported above is the SPH-based solver known as DualSPHysics (Domínguez et al., 2022), which also constitutes the core of the present paper. By means of a fully Lagrangian environment and couplings with external libraries (Domínguez et al., 2019; Martínez-Estévez et al., 2023a; Martínez-Estévez et al., 2023b), DualSPHysics offers powerful support for multi-physics high-fidelity simulations of floating structures. In this work, employing the external library MoorDynPlus (Domínguez et al., 2019), the novel mooring layout proposed in Niosi et al. (2024) for the DeepCwind platform is considered as ground-truth; reference data is available in an open-source repository at Niosi et al. (2023b).

This study focuses on investigating the hydrodynamic response of a semi-submersible sub-structure that hosts a 5-MW wind turbine. Specifically, the DeepCWind model from the OC5 project (Robertson et al., 2014) was considered. As opposed to the purpose of the OC5 project, in Niosi et al. (2023b), the vessel was used as a benchmark platform to test a novel mooring configuration, intended for the Mediterranean Sea, and set through a multi-parameter optimization tool base on a Matlab–Orcaflex framework (Ghigo et al., 2022), similarly to what is proposed in West et al. (2021), with prior successful applications (Niosi et al., 2023a; Bertozzi et al., 2024). The SPH model we propose to predict the response of a DeepCwind platform with an innovative mooring configuration has revealed promising, correctly capturing flow-induced features generated by wave–structure interaction. In addition, it is also concluded that higher numerical resolution is required to enhance model outcomes at lower frequencies.

2 SPH MODEL

SPH is based on the discretization of Navier–Stokes equations in correspondence to a set of computational nodes (particles), in which they are integrated based on the physical properties of the surrounding particles (Violeau & Rogers, 2016). To determine the neighbors' contributions of a given particle a, a kernel function W_{ab} and its compact support radius $(2h)$ are defined.

2.1 *Governing equations*

The momentum equation in SPH formalism can be rewritten as:

$$\frac{D\boldsymbol{v}_a}{Dt} = -\sum_{b=1}^{N_p} m_b \left(\frac{P_b + P_a}{\rho_a \rho_b}\right) \cdot \nabla_a W_{ab} + \boldsymbol{g} + \mathcal{L}, \quad (1)$$

where P is the pressure, ρ is the density and $\mathcal{L}$ represents the laminar viscosity term as introduced by Lo & Shao (2002).

The continuity equation instead can be expressed as:

$$\frac{d\rho_a}{dt} = \rho_a \sum_b \frac{m_b}{\rho_b} \mathbf{v}_{ab} \cdot \nabla_a W_{ab} + \\ + \delta h c_s \sum_b \Psi_{ab} \cdot \nabla_a W_{ab} \frac{m_b}{\rho_b} \quad (2)$$

where the right hand term introduces density diffusion (Molteni & Colagrossi, 2009; Fourtakas et al., 2019) to reduce the density fluctuations. As DualSPHysics treats the fluid as weakly compressible, an additional equation of state is used to relate pressure and density. It goes:

$$P_a = \frac{c^2 \rho_0}{\gamma} \left[\left(\frac{\rho_a}{\rho_0} \right)^{\gamma} - 1 \right], \tag{3}$$

where ρ_0 is the reference density, c is the speed of sound at the reference density and γ is the polytropic constant, usually set to 7. For an exhaustive description of the numerical scheme, the reader may refer to Domínguez et al. (2022).

2.2 *Boundary conditions*

The modified dynamic boundary conditions (mDBC) (English et al., 2022), are implemented in this work. This approach builds upon the DBC presented in Crespo et al. (2007), as the original version was affected by non-physical forces developed at the interface as a consequence of the repulsive force created by the increasing density of the approaching fluid particle. This often resulted in large gaps between the boundary and the first fluid particles layer, and spurious pressure field (Domínguez et al., 2015), which is now avoided with the mDBC approach. Further information and applications for various kinds of WSI can be found in Mitsui et al. (2023) and Ruffini et al. (2021).

3 NUMERICAL SETUP

3.1 *Reference case*

The DeepCwind platform geometry adheres to the design proposed in Robertson et al. (2014) and corresponds to a $1:96$ scale model (refer to Figure 2). Constructed from PVC, the model features 125 mm pipes for the surface piercing columns and 250 mm pipes for the heave plates. Very thin steel rods connect the outer columns to the inner column at the top and bottom, supplemented by three inclined rods for added shear stiffness. The properties of the overall platform configuration are reported in Table 1. A much detailed description regarding the model construction and specifications can be found in Metsch (2023).

Testing was carried out in the Towing Tank 2 of the Ship Hydromechanics Laboratory of Delft University of Technology (The Netherlands), using a wave tank 85 meters long, 2.76 meters wide, and with 1.04-meter water depth. The platform, as kept at station by the mooring system, is shown in Figure 1. A flap-type wavemaker with an adjustable virtual hinge point was used for the generation of customized wave trains. Herein, only long-crested regular waves are considered, and used for this numerical validation. Table 2

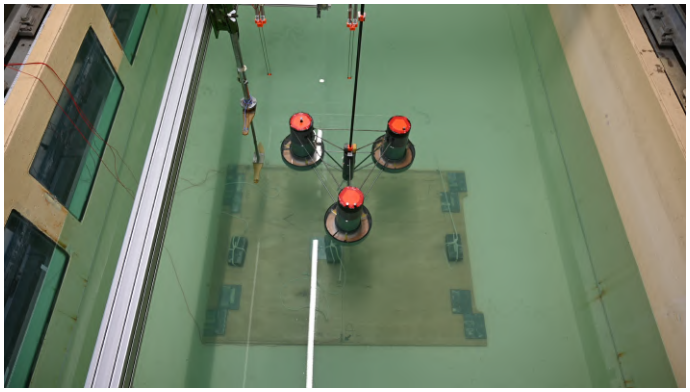

Figure 1: Photographic view of the platform at the Towing Tank 2 of the Ship Hydromechanics Laboratory of Delft University of Technology (The Netherlands). Reproduced from Niosi et al. (2024).

Table 1: Geometrical and mechanical properties in a body-fixed coordinate system.

Mass: M_P[kg]	15.90
CoG_P (x, y, z) [m]	(0.0, 0.0, 0.128)
Draft [m]	0.21
Nominal width [m]	0.64
Nominal breadth [m]	0.73
I_{xx} [kg m^2]	1.772
I_{yy} [kg m^2]	1.788
I_{zz} [kg m^2]	1.22

tags the nine wave conditions excerpted from the experimental dataset. Their frequency property are defined such that the first six cover a spectrum wide enough to contain the heave peak period, whereas the last three, repeat OP_1, OP_3, and OP_6 but having greater steepness, computed as the ratio between the wave height over the wave length.

Table 2: Regular wave description.

ID	**H (mm)**	**T (s)**	**Steepness (H/λ)**
OP_1	11.70	0.61	1/30
OP_2	15.90	0.71	1/30
OP_3	20.80	0.82	1/30
OP_4	26.30	0.92	1/30
OP_5	32.51	1.02	1/30
OP_6	46.81	1.22	1/30
OP_7	17.60	0.61	1/25
OP_8	31.20	0.82	1/25
OP_9	70.02	1.22	1/25

3.2 *Mooring setup*

The mooring system comprises three inclined tendons that at equilibrium display pretension to counter the platform excess of buoyancy. As mentioned, the configuration used for this work corresponds to the solution of multi-parameter optimization tool based on a Matlab–OrcaFlex framework (Ghigo et al., 2022), which targeted minimizing the overall costs of the lines and thereby the anchoring system. Herein, among the proposed configurations tested in Niosi et al. (2024), the layout configuration with springs and

polyester lines is used for the validations aimed by this work. Several elements were used to achieve the most realistic modeling for the physical tests, however here, some simplifications are applied, which are summarized by the schematic view proposed in Figure 2.

It is handled by the dynamic solver MoorDynPlus (Domínguez et al., 2019). Table 3 lists the main parameters that are used to set up the line properties in the numerical model and the solver time step. According to the reference research paper, the test in which the system was kept linear concentrates the deformation into the element tagged as "Springs", whereas the polyester lines contribute none to the overall extensional response and acted as mere connections. This reflects here as the stiffness of the polyester lines is just set as to be big enough to avoid meaningful line deformation. Hence, the system response is dominated by the compliance of the spring element. A preliminary still-water test was performed to ensure the line tension at rest, which has yielded close agreement to the reference pretension value of 1.78 N (average among the three lines) applied during the testing.

Table 3: Input parameters used for the definition of the springs.

Spring	
Stiffness: K_l [N]	30.4
Nominal diameter: D_N [mm]	0.0036
Length: L_0 [m]	0.032
Segments: N [-]	7
Density in air: ρ [kg/m^3]	7500
Distributed mass: ρ_l [kg/m]	0.01
Polyester	
Stiffness: K_l [N]	5000
Nominal diameter: D_N [mm]	0.00012
Segments: N [-]	7
Density in air: ρ [kg/m^3]	1200
Distributed mass: ρ_l [kg/m]	0.0017
Model parameters	
Time step: dt_M [s]	2e-05

Table 4: Mass properties in a body-fixed coordinate system.

Mass: M$_P$[kg]	15.90
CoG$_P$ (x, y, z) [m]	(0.0, 0.0, 0.128)
Draft [m]	0.21
Nominal width [m]	1.26
Nominal breadth [m]	1.44
I$_{xx}$ [kg m^2]	1.772
I$_{yy}$ [kg m^2]	1.788
I$_{zz}$ [kg m^2]	1.220

4 NUMERICAL VALIDATION

Herein, following the modeling methodology adopted in Tagliafierro et al. (2023b), the initial inter-particle distance, dp, is taken as proportional to the thickness of the heave plate, H$_P$=0.062 m. Specifically, two resolutions, H$_P$/5 and H$_P$/10 are considered, respectively, to identify the dynamic properties of the moored platforms, whereas only the first one, H$_P$/5, is considered to study the wave–solid structure interaction.

Table 5: Fairlead and anchor position of the mooring lines at equilibrium.

Description	**Connection**	**x** [m]	**y** [m]	**z** [m]
Fore	Fairlead	-0.426	0.00	-0.146
	Anchor	-0.781	0.000	-1.042
Starboard	Fairlead	0.213	-0.369	-0.146
	Anchor	0.381	0.678	-1.042
Port	Fairlead	0.213	-0.369	-0.146
	Anchor	0.381	0.678	-1.042

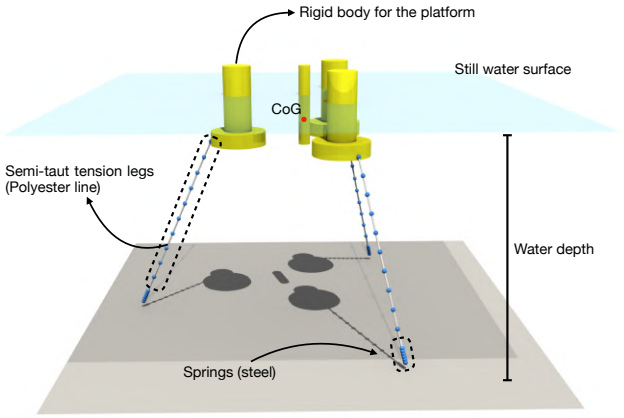

Figure 2: Overview of the numerical setup for the decay test.

4.1 *Heave decay test*

A first benchmark for this numerical model consists of a heave decay test, which here is considered as the most representative way to stress the axial stiffness of the taut lines. Reference is made to an initial configuration which features a 0.060 m displacement along the fore side. Note that for a similar platform configuration Tagliafierro et al. (2023b) performed a convergence study for the heave decay test. However, as the mooring configuration differs, this initial testing is deemed necessary to ensure model correctness.

Figure 3 contrasts the numerical outcomes against the reference time series. Both resolutions exhibit noticeable agreement, however, with different degrees of accuracy; the coarser, H$_P$/5, behaves very well in frequency and amplitude up to the third cycle, whence an increase in damping occurs. Instead, the finer, H$_P$/10, apart from a slight overestimation on the peaks in the first loops, consistently predicts both amplitude and period of the vertical oscillations throughout the whole test. It is worth including some details here regarding the physical testing that may make the model deviate from the intended layout. First, the decay test

was performed in a wave tank, which has finite width and was not fitted with any anti-reflective layer. For the numerical setup, a theoretical infinite size of the tank is assumed with proper treatment to avoid boundary wall reflection. Secondly, small deviation in the positioning of the mooring lines and accidental eccentricity in the definition of the platform CoG may give rise to coupled effects within modes. Thus, keeping in mind these two points can surely help frame the quality of the results just presented in this section.

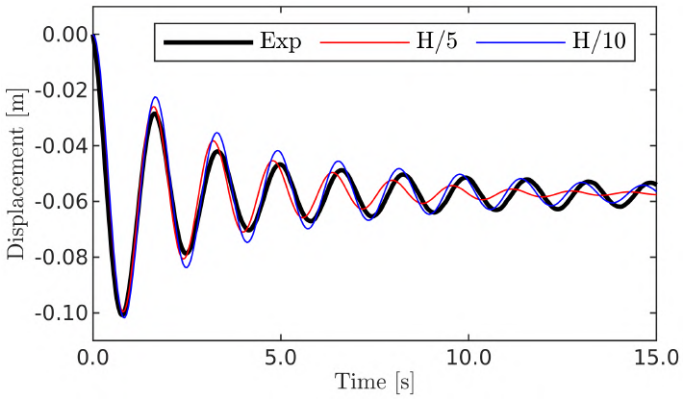

Figure 3: Heave decay test for the moored platform, with two different SPH resolutions.

4.2 *Response amplitude operator*

To begin with, the numerical setup that handles wave generation and propagation is described. A flat-bottom flume is considered with water depth (i.e., 1.04 m) corresponding to the physical tank. Generation is accomplished by a piston-type wavemaker equipped with an active wave absorption system (AWAS), following the implementation proposed in Altomare et al. (2017), which includes a control routine over the generated incident wave. Such a piston comprises moving boundary particles. Although smaller than the physical tank (i.e., width 4.22 m), the tank width is taken as twice the nominal width of the platform, which has proven sufficient to ensure accurate results. The tank has a parametric length, in an attempt to mediate accuracy and computational runtime. As opposed to the 142.00 m of the physical tank, the length of numerical fluid domain before the platform rest-position is proportional to the wavelength being generated; the latter, L_i is computed by solving the dispersion formula. Ultimately, to prevent lateral reflection, the width is set to twice the apparent diameter of the floater in conjunction with numerical damping bands 10-cm wide on the lateral edges. Note that for the following investigation, the numerical model employs the particle size dp=H$_P$/5.

For estimating the RAO, a total of nine wave conditions are considered. The wave parameters used to form the RAOs are provided in Table 2. These wave conditions cover a range from linear to non-linear waves, also including different wave steepness values, as easily rendered by Figure 4. To evaluate the RAO, for each simulation, the motion amplitude corresponding to the degree of freedom of interest is gauged from a frequency-domain decomposition. It is then divided by the wave amplitude of the incident wave, computed from another simulation where pure wave propagation is assumed. The results are then arranged into Figure 5.

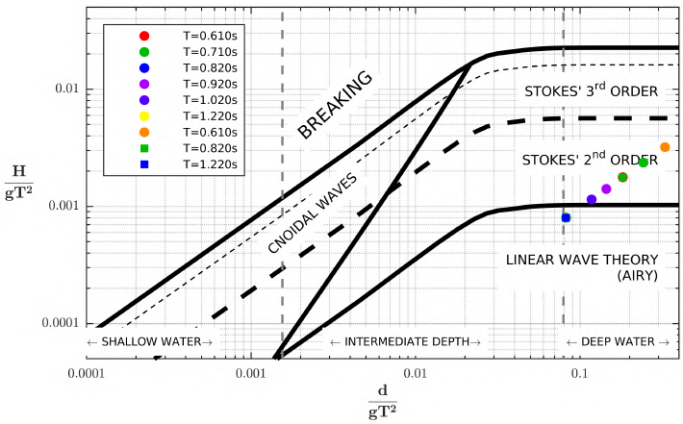

Figure 4: Regular wave classification.

Figure 5 shows the RAO for the surge and heave degree of freedom, which is compared with reference solutions. The first chart, reporting the surge RAO comparison, reveals quite good agreement throughout the frequency spectrum, as the overall behavior is captured with errors within a few percent of the references. When running waves of different steepness, the model predicts the system non-linearity induced by greater forcing agents. In the high-frequency (low-period) region, steeper waves do not significantly hit the surge motion, indicating an almost linear response of the system. However, as the wave frequency lowers (increased period values), such divide becomes increasingly higher, as it is demonstrated by the markers corresponding to OP_6 and OP_9. Again, the model captures this increased non-linearity between the forcing term and the surge displacement.

The second panel in Figure 5 shows the RAO for the heave motion. Overall, very good agreement can be noticed although some markers reveal slight misprediction. Specifically, for high frequencies the model fails to correctly predict the heave RAO with high discrepancy between the cases that account for different wave steepness. This is however to be expected given the very small simulated wave height, which requires better resolution to be correctly generated and propagated. On the other hand, for low frequencies, the model is accurate but not precise. As it has been observed for the surge RAO, the model correctly captures the changes in hydrodynamics when the wave height is changed. This time, however, the RAO is slightly underestimated. Possible causes of mismatching could be generated here by some difference in the hydrodynamic heave stiffness.

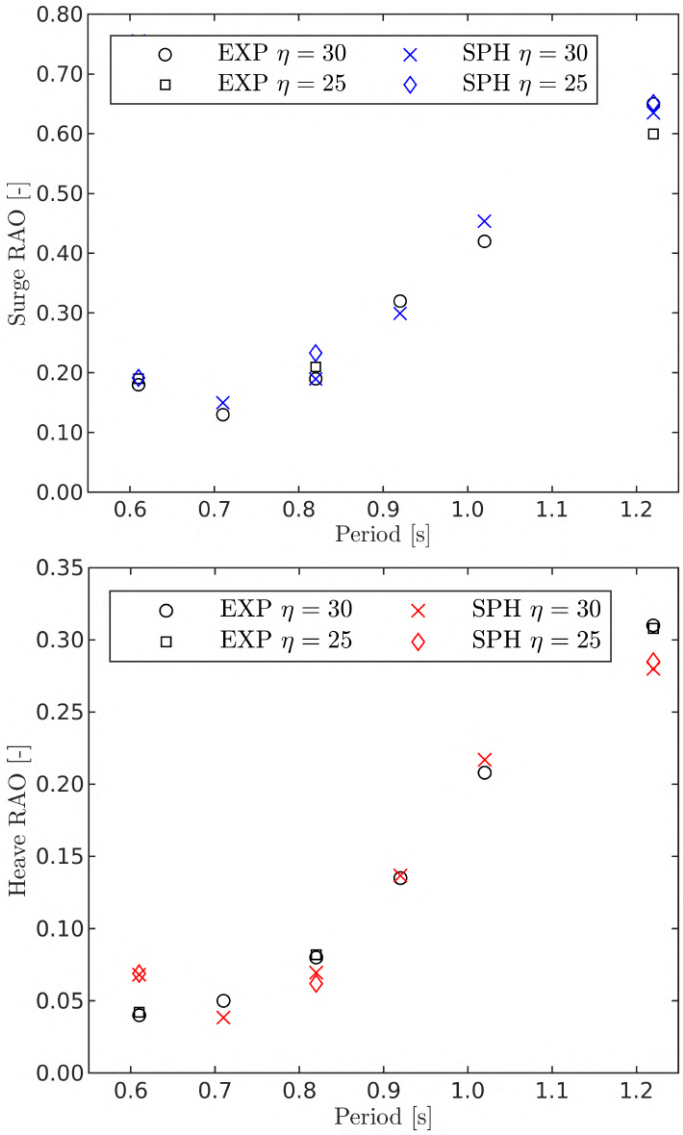

Figure 5: RAO response in heave and surge. η indicates the wave steepness as H/λ.

5 CONCLUSIONS

We have presented a numerical model validation for an SPH-based solver grounded on predicting the dynamic response of a semi-submersible platform under regular wave excitation. A preliminary model validation has been performed using a heave decay test. It was revealed that the proposed model setup can capture the properties of the mooring system, which dominates here, quite well for a first resolution dp=H$_P$/5, and very well when more particles, corresponding to dp=H$_P$/10, are used. For the latter resolution, its prediction fits frequency and damping response. Finally, an RAO analysis has been used to qualitatively ascertain the model accuracy. The proposed setup proved quite reliable in predicting the motion of the DeepCwind platform under regular waves, showing good matching for the surge RAO, whereas some loss of precision is shown for the heave RAO. However, the most important outcome of the presented validation comes from the capability that the model has shown in predicting changes in the system behavior when different wave steepness are considered, proving how high-fidelity models are "predictive" and could be potentially employed up to very high TRL (technology readiness level) levels during the development of novel concepts for renewable energy devices, such as the one proposed here.

CFD models can provide levels of accuracy that are comparable to real expectations in simulating operative conditions, expressly when the latter conditions entail coupled effects among the various components that characterize the dynamics of structures at sea for renewable energy. As of now, viscosity and turbulence still configure fields under investigation within the SPH community, as remarked in Vacondio et al. (2020), but, nonetheless, investing research effort in DualSPHysics is deemed relevant. This simulation platform can also tackle the hydroelastic analysis of the various components of the floating platforms (O'Connor & Rogers, 2021) (posited as well by the novel OC7 project) or account for the dynamics of the wind towers and rotor blades (Capasso et al., 2022; Martínez-Estévez et al., 2023b), whereas more realistic hydrodynamic investigations could be made possible by the implementation of more comprehensive environmental loads, such as combinations of waves and currents (Capasso et al., 2023; Yang et al., 2023; Yang et al., 2024).

ACKNOWLEDGEMENTS

We are grateful for the use of the computing resources from the Northern Ireland High Performance Computing (NI-HPC) service funded by EPSRC (EP/T022175). This work was partially financed by the Ministeiro de Ciencia e Innovación of the Government of Spain under project "SURVIWEC PID2020-113245RB-I0" and financed by Xunta de Galicia, Consellería de Cultura, Educación e Universidade, under project ED431C 2021/44 "Programa de Consolidación e Estructuración de Unidades de Investigación Competitivas", under grant TED2021-129479A-I00 funded by MCIN/AEI/ 10.13039/501100011033 and by "European Union NextGenerationEU/PRTR" and under grant CNS2022-136073 funded by MCIN/AEI/ 10.13039/501100011033 and by "European Union NextGenerationEU/PRTR".

I. Martínez-Estévez acknowledges funding from Xunta de Galicia under "Programa de axudas á etapa predoutoral da Consellería de Cultura, Educación e Universidades da Xunta de Galicia" (ED481A-2021/337). J. Domínguez acknowledges funding from grant RYC2022-038341-I funded by MCIN/AEI/ 10.13039/501100011033 and by "ESF Investing in your future".

DATA AVAILABILITY STATEMENT

Data sets generated during the current study are available from the corresponding author upon reasonable request.

REFERENCES

Altomare, C., J. Domínguez, A. Crespo, J. González-Cao, T. Suzuki, M. Gómez-Gesteira, & P. Troch (2017). "Long-crested wave generation and absorption for SPH-based DualSPHysics model". In: *Coastal Engineering* 127, pp. 37–54.

Antonutti, R., C. Peyrard, L. Johanning, A. Incecik, & D. Ingram (2014). "An investigation of the effects of wind-induced inclination on floating wind turbine dynamics: heave plate excursion". In: *Ocean Engineering* 91, pp. 208–217.

Bertozzi, A., F. Niosi, X. Jiang, & Z. Jiang (2024). "Numerical Calibration of the Mooring System for a Semi-Submersible Floating Wind Turbine Model". In: *Journal of Offshore Mechanics and Arctic Engineering* 146.6.

Capasso, S., B. Tagliafierro, I. Martínez-Estévez, J. Domínguez, A. Crespo, & G. Viccione (2022). "A DEM approach for simulating flexible beam elements with the Project Chrono core module in DualSPHysics". In: *Computational Particle Mechanics*.

Capasso, S., B. Tagliafierro, S. Mancini, I. Martínez-Estévez, C. Altomare, J. M. Domínguez, & G. Viccione (2023). "Regular Wave Seakeeping Analysis of a Planing Hull by Smoothed Particle Hydrodynamics: A Comprehensive Validation". In: *Journal of Marine Science and Engineering* 11.4.

Crespo, A., M. Gómez-Gesteira, & R. Dalrymple (2007). "Boundary conditions generated by dynamic particles in SPH methods". In: *Computers, Materials and Continua* 5.3, pp. 173–184.

Crespo, A. et al. (2023). "On the state-of-the-art of CFD simulations for wave energy converters within the open-source numerical framework of DualSPHysics". In: *Proceedings of the European Wave and Tidal Energy Conference* 15.

Davidson, J. & R. Costello (2020). "Efficient Nonlinear Hydrodynamic Models for Wave Energy Converter Design—A Scoping Study". In: *Journal of Marine Science and Engineering* 8.1.

Domínguez, J. M. et al. (2022). "DualSPHysics: from fluid dynamics to multiphysics problems". In: *Computational Particle Mechanics* 9.5, pp. 867–895.

Domínguez, J., A. Crespo, M. Hall, C. Altomare, M. Wu, V. Stratigaki, P. Troch, L. Cappietti, & M. Gómez-Gesteira (2019). "SPH simulation of floating structures with moorings". In: *Coastal Engineering* 153, p. 103560.

Domínguez, J., A. Crespo, & e. a. Fourtakas G (2015). "Evaluation of reliability and efficiency of different boundary conditions in an SPH code". In: *Proceedings of the 10th international SPHERIC workshop*, pp. 341–348.

English, A., J. Domínguez, R. Vacondio, A. Crespo, P. Stansby, S. Lind, L. Chiapponi, & M. Gómez-Gesteira (2022). "Modified dynamic boundary conditions (mDBC) for general-purpose smoothed particle hydrodynamics (SPH): application to tank sloshing, dam break and fish pass problems". In: *Computational Particle Mechanics* 9.5, pp. 1–15.

Faraggiana, E., G. Giorgi, M. Sirigu, et al. (2022). "A review of numerical modelling and optimisation of the floating support structure for offshore wind turbines". In: *Journal of Ocean Engineering and Marine Energy* 8, pp. 433–456.

Fourtakas, G., J. M. Dominguez, R. Vacondio, & B. D. Rogers (2019). "Local uniform stencil (LUST) boundary condition for arbitrary 3-D boundaries in parallel smoothed particle hydrodynamics (SPH) models". In: *Computers & Fluids* 190, pp. 346–361.

Ghigo, A., F. Niosi, B. Paduano, G. Bracco, & G. Mattiazzo (2022). "Mooring System Design and Analysis for a Floating Offshore Wind Turbine in Pantelleria". In: vol. Volume 11: Wind Energy. Turbo Expo: Power for Land, Sea, and Air, V011T38A021.

Jonkman, J. M., M. L. Buhl, et al. (2005). *FAST user's guide*. Vol. 365. National Renewable Energy Laboratory Golden, CO, USA.

Katsidoniotaki, E., Z. Shahroozi, C. Eskilsson, J. Palm, J. Engström, & M. Göteman (2023). "Validation of a CFD model for wave energy system dynamics in extreme waves". In: *Ocean Engineering* 268, p. 113320.

Lauria, A., P. Loprieno, A. Francone, E. Leone, & G. Tomasicchio (2024). "Recent advances in understanding the dynamic characterization of floating offshore wind turbines". In: *Ocean Engineering* 307.

Lo, E. & S. Shao (2002). "Simulation of near-shore solitary wave mechanics by an incompressible SPH method". In: *Applied Ocean Research* 24, pp. 275–286.

Martínez-Estévez, I., J. M. Domínguez, B. Tagliafierro, R. B. Canelas, O. García-Feal, A. J. C. Crespo, & M. Gómez-Gesteira (2023a). "Coupling of an SPH-based solver with a multiphysics library". In: *Computer Physics Communications* 283, p. 108581.

Martínez-Estévez, I., B. Tagliafierro, J. El Rahi, J. Domínguez, A. Crespo, P. Troch, & M. Gómez-Gesteira (2023b). "Coupling an SPH-based solver with an FEA structural solver to simulate free surface flows interacting with flexible structures". In: *Computer Methods in Applied Mechanics and Engineering* 410, p. 115989.

Metsch, Y. (2023). *Experimental low frequency mooring analysis of a floating offshore wind turbine*. Delft University of Technology.

Mitsui, J., C. Altomare, A. J. Crespo, J. M. Domínguez, I. Martínez-Estévez, T. Suzuki, S. Kubota, & M. Gómez-Gesteira (2023). "DualSPHysics modelling to analyse the response of Tetrapods against solitary wave". In: *Coastal Engineering* 183, p. 104315.

Molteni, D. & A. Colagrossi (2009). "A simple procedure to improve the pressure evaluation in hydrodynamic context using the SPH". In: *Computer Physics Communications* 180.6, pp. 861–872.

Niosi, F., E. Begovic, C. Bertorello, B. Rinauro, G. Sannino, M. Bonfanti, & S. A. Sirigu (2023a). "Experimental validation of Orcaflex-based numerical models for the PEWEC device". In: *Ocean Engineering* 281, p. 114963.

Niosi, F., O. Dell'Edera, & S. Schreier (2023b). *Experimental Dataset of taut-leg mooring system for FOWT*.

Niosi, F., O. Dell'Edera, M. Glorioso, G. Giorgi, & S. Schreier (2024). "Experimental Investigation and Dataset Release of a Taut-Leg Mooring System for a Semi-Submersible Floating Offshore Wind Turbine". In: *Marine Structure*.

Niosi, F., O. Dell'edera, M. Sirigu, A. Ghigo, & G. Bracco (2023c). "A Comparison Between Different Numerical Models and Experimental Tests for the Study of Floating Offshore Wind Turbines". In: pp. 382–389.

O'Connor, J. & B. D. Rogers (2021). "A fluid–structure interaction model for free-surface flows and flexible structures using smoothed particle hydrodynamics on a GPU". In: *Journal of Fluids and Structures* 104, p. 103312.

Paduano, B., L. Parrinello, F. Niosi, O. Dell'Edera, S. A. Sirigu, N. Faedo, & G. Mattiazzo (2024). "Towards standardised design of wave energy converters: A high-fidelity modelling approach". In: *Renewable Energy*, p. 120141.

Pribadi, A., L. Donatini, E. Lataire, G. Verao Fernandez, & I. Martínez-Estévez (2023). "Validation of a computationally efficient time-domain numerical tool against DeepCwind experimental data". In: ed. by S. C.G. CRC Press/Balkema, pp. 597–608.

Ransley, E., D. Greaves, A. Raby, D. Simmonds, & M. Hann (2017). "Survivability of wave energy converters using CFD". In: *Renewable Energy* 109, pp. 235–247.

Robertson, A. N. et al. (2020). "OC6 Phase I: Investigating the underprediction of low-frequency hydrodynamic loads and responses of a floating wind turbine". In: *Journal of Physics: Conference Series* 1618.3, p. 032033.

Robertson, A., J. Jonkman, M. Masciola, H. Song, A. Goupee, A. Coulling, & C. Luan (2014). "Definition of the Semisubmersible Floating System for Phase II of OC4". In.

Robertson, A. & L. Wang (2021). "OC6 Phase Ib: Floating Wind Component Experiment for Difference-Frequency Hydrodynamic Load Validation". In: *Energies* 14.19.

Robertson, A. N. et al. (2017). "OC5 Project Phase II: Validation of Global Loads of the DeepCwind Floating Semisubmersible Wind Turbine". In: *Energy Procedia* 137, pp. 38–57.

Ruffini, G., R. Briganti, P. De Girolamo, J. Stolle, B. Ghiassi, & M. Castellino (2021). "Numerical Modelling of Flow-Debris Interaction during Extreme Hydrodynamic Events with DualSPHysics-Chrono". In: *Applied Sciences* 11.8.

Salis, N., X. Hu, M. Luo, A. Reali, & S. Manenti (2024). "3D SPH analysis of focused waves interacting with a floating structure". In: *Applied Ocean Research* 144, p. 103885.

Shi, W., L. Zhang, M. Karimirad, C. Michailides, Z. Jiang, & X. Li (2023). "Combined effects of aerodynamic and second-order hydrodynamic loads for floating wind turbines at different water depths". In: *Applied Ocean Research* 130.

Tagliafierro, B., S. Capasso, I. Martínez-Estévez, M. Göteman, H. Bernhoff, M. Karimirad, J. Domínguez, C. Altomare, G. Viccione, A. Crespo, & M. Gómez-Gesteira (2023a). "Hydrodynamic validation of a semi-submersible floating platform supporting a 15MW wind turbine toweunder extreme loading scenarios with DualSPHysics and MoorDyn+". In: International Society of Offshore and Polar Engineers, pp. 218–226.

Tagliafierro, B., M. Karimirad, C. Altomare, M. Göteman, I. Martínez-Estévez, S. Capasso, J. M. Domínguez, G. Viccione, M. Gómez-Gesteira, & A. J. Crespo (2023b). "Numerical validations and investigation of a semi-submersible floating offshore wind turbine platform interacting with ocean waves using an SPH framework". In: *Applied Ocean Research* 141, p. 103757.

Tagliafierro, B., M. Karimirad, S. Capasso, M. Göteman, I. Martínez-Estévez, J. M. Domínguez, C. Altomare, G. Viccione, A. J. Crespo, & D. Negrut (2023c). "Coupled numerical simulation of floating offshore wind turbine platforms: investigating the effects of wave and wind loading using a high-fidelity SPH-based model". In: American Society of Mechanical Engineers (ASME).

Tagliafierro, B., M. Karimirad, I. Martínez-Estévez, J. M. Domínguez, G. Viccione, & A. J. C. Crespo (2022a). "Numerical Assessment of a Tension-Leg Platform Wind Turbine in Intermediate Water Using the Smoothed Particle Hydrodynamics Method". In: *Energies* 15.11.

Tagliafierro, B., I. Martínez-Estévez, J. M. Domínguez, A. J. Crespo, M. Göteman, J. Engström, & M. Gómez-Gesteira (2022b). "A numerical study of a taut-moored point-absorber wave energy converter with a linear power take-off system under extreme wave conditions". In: *Applied Energy* 311, p. 118629.

Tan, Z., P.-N. Sun, N.-N. Liu, Z. Li, H.-G. Lyu, & R.-H. Zhu (2023). "SPH simulation and experimental validation of the dynamic response of floating offshore wind turbines in waves". In: *Renewable Energy* 205, pp. 393–409.

Vacondio, R., C. Altomare, M. Leffe, X. Hu, D. Le Touzé, S. Lind, J.-C. Marongiu, S. Marrone, B. Rogers, & A. Souto-Iglesias (2020). "Grand challenges for Smoothed Particle Hydrodynamics numerical schemes". In: *Computational Particle Mechanics* 8, pp. 1–14.

Violeau, D. & B. Rogers (2016). "Smoothed particle hydrodynamics (SPH) for free-surface flows: past, present and future". In: *Journal of Hydraulic Research* 54.1, pp. 1–26.

Wang, L., A. Robertson, J. Kim, H. Jang, Z.-R. Shen, A. Koop, T. Bunnik, & K. Yu (2022). "Validation of CFD simulations of the moored DeepCwind offshore wind semisubmersible in irregular waves". In: *Ocean Engineering* 260, p. 112028.

Wang, L. et al. (2021). "OC6 Phase Ib: Validation of the CFD predictions of difference-frequency wave excitation on a FOWT semisubmersible". In: *Ocean Engineering* 241, p. 110026.

West, W., A. Goupee, S. Hallowell, & A. Viselli (2021). "Development of a Multi-Objective Optimization Tool for Screening Designs of Taut Synthetic Mooring Systems to Minimize Mooring Component Cost and Footprint". In: *Modelling* 2.4, pp. 728–752.

Windt, C., J. Davidson, & J. V. Ringwood (2018). "High-fidelity numerical modelling of ocean wave energy systems: A review of computational fluid dynamics-based numerical wave tanks". In: *Renewable and Sustainable Energy Reviews* 93, pp. 610–630.

Yang, Y., S. Draycott, P. K. Stansby, & B. D. Rogers (2023). "A numerical flume for waves on variable sheared currents using smoothed particle hydrodynamics (SPH) with open boundaries". In: *Applied Ocean Research* 135, p. 103527.

Yang, Y., A. English, B. D. Rogers, P. K. Stansby, D. Stagonas, E. Buldakov, & S. Draycott (2024). "Numerical modelling of a vertical cylinder with dynamic response in steep and breaking waves using smoothed particle hydrodynamics". In: *Journal of Fluids and Structures* 125, p. 104049.

Zhang, W., J. Calderon-Sanchez, D. Duque, & A. Souto-Iglesias (2024). "Computational Fluid Dynamics (CFD) applications in Floating Offshore Wind Turbine (FOWT) dynamics: A review". In: *Applied Ocean Research* 150, p. 104075.